Interfacial Charge Engineering in TiSSe/Borophene van der Waals Heterostructures for Enhanced Quantum Capacitance and Electro-Mechanical Stability

Sandriya Teresa Raju C[1], Saumyashree Das[1], Mangal S. Yadav[1], Laxmi Mehra[1], A. L. Sharma[1*]

[1] Department of Physics, Central University of Punjab, Bathinda, Punjab, India – 151401

* Corresponding author: alsharma@cup.edu.in

Supporting Information

Stacking configurations

Stacking configurations as shown in **Figs. S1 and S2** were considered during stacking screening to identify structurally stable vdW heterostructures. However, lower binding energy configurations were excluded due to severe borophene distortion and non-vdW-like interlayer bonding, as observed from structural relaxation.

Table S1. Summary of investigated stacking configurations for TiSSe/H-borophene heterostructure for S-B and Se-B interfaces.

Interface	Initial B position	Binding energy	Interlayer distance (Å)	Structural outcome	Considered for analysis
S–B	Hollow / bridge	Reference	2.76100	Stable, minor borophene distortion	Yes
S–B	On top of S	Lower	1.89175	Significant borophene distortion.	No
S–B	On top of Ti	Lower	1.8915	Relaxes to B-on-S, distorted	No
Se–B	Hollow / bridge	Reference	3.25703	Stable, no borophene distortion	Yes
Se–B	On top of Se	Lower	2.03014	Significant borophene	No

				distortion	
Se–B	On top of Ti	Lower	2.06929	Relaxes to B-on-Se, distorted	No

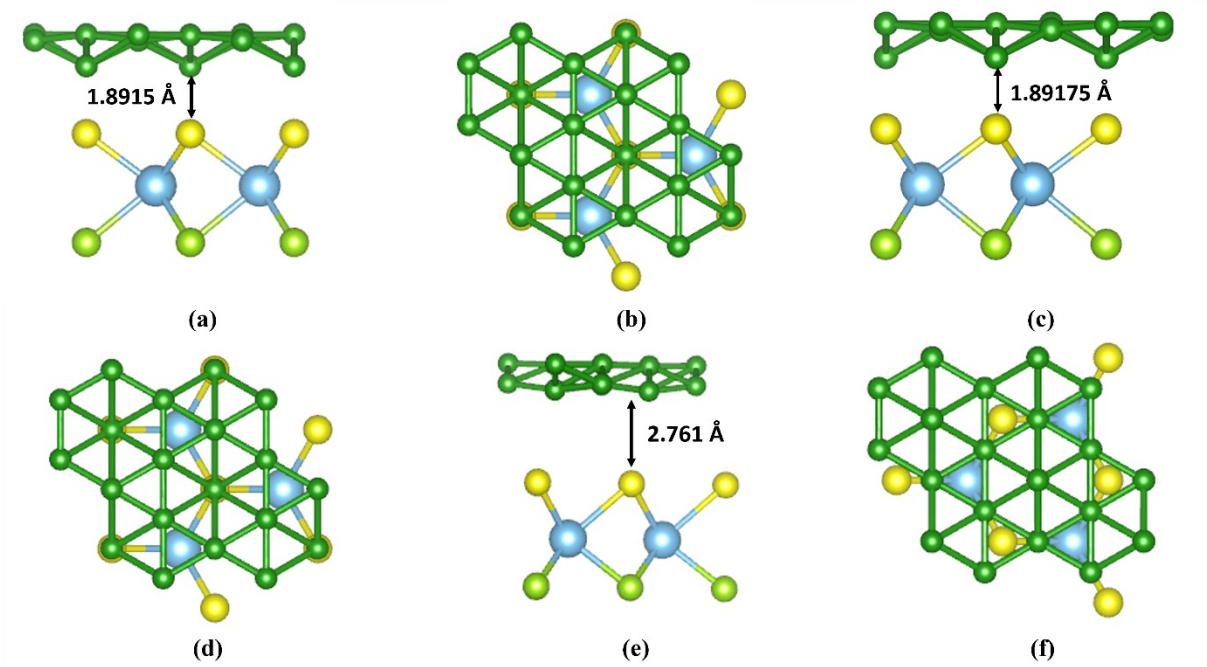

Fig. S1. Side and top views of the TiSSe/H-borophene heterostructure showing various stacking configurations for the S–B interface, including B atoms positioned **(a, b)** above Ti atoms, **(c, d)** S atoms, and **(e**, **f)** hollow/bridge sites.

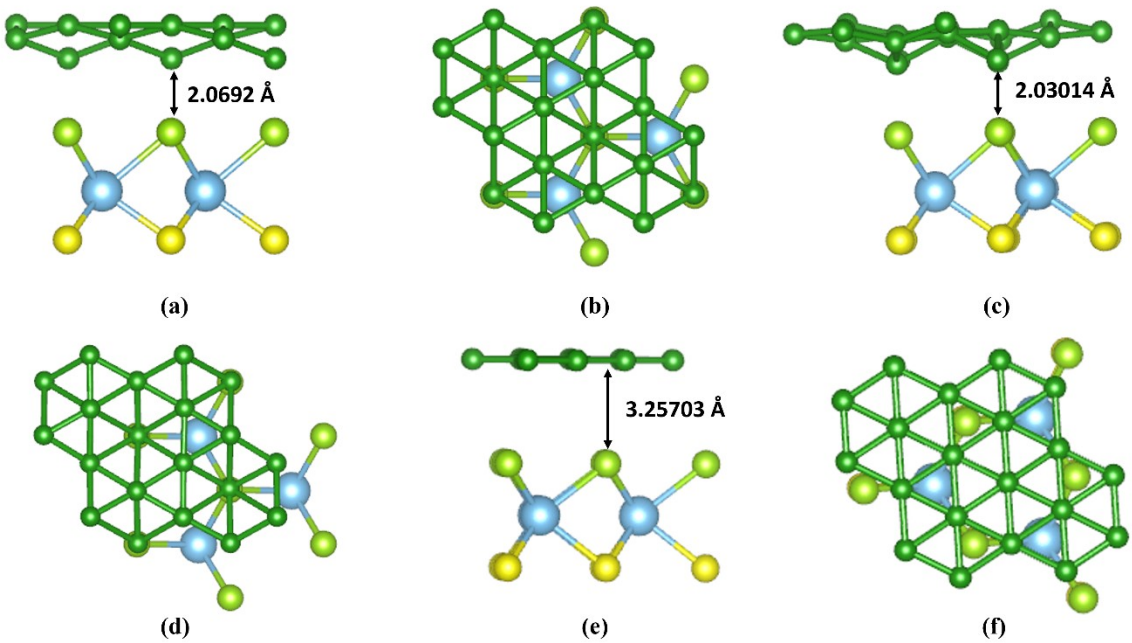

Fig. S2. Side and top views of the TiSSe/H-borophene heterostructure showing various stacking configurations for the Se–B interface, including B atoms positioned **(a, b)** above Ti atoms, **(c, d)** S atoms, and **(e**, **f)** hollow/bridge sites. These configurations were considered during stacking screening to identify structurally stable vdW heterostructures.

2. AIMD calculations

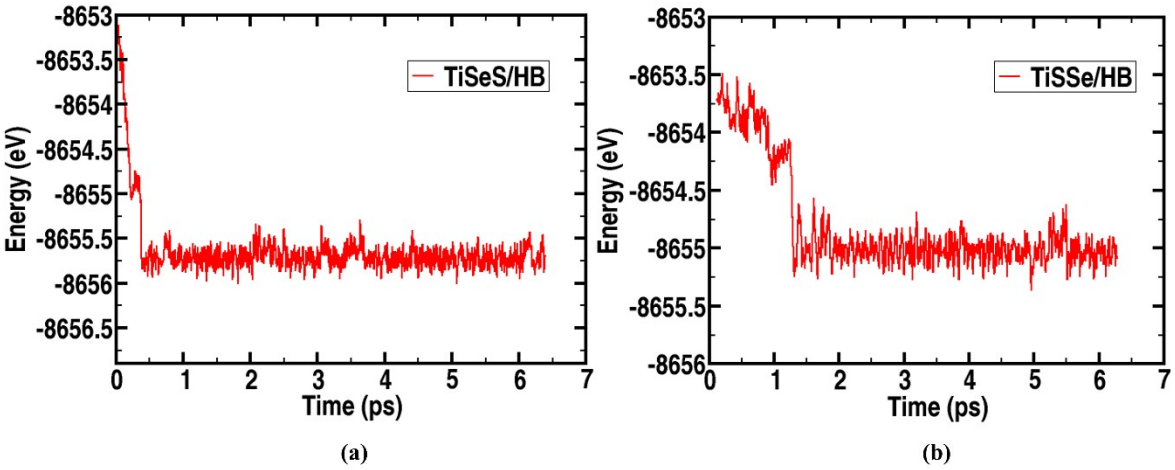

Fig. S3. Variation of energy as a function of simulation time during AIMD run at 300 K of **(a)** S-B interface and **(b)** Se-B interface of TiSSe/H-borophene heterostructure.

3. Transport properties

To clarify the origin of carrier polarity and strengthen the thermoelectric discussion, transport properties of pristine-Janus monolayer and H-borophene were evaluated within the same BoltzTraP framework.

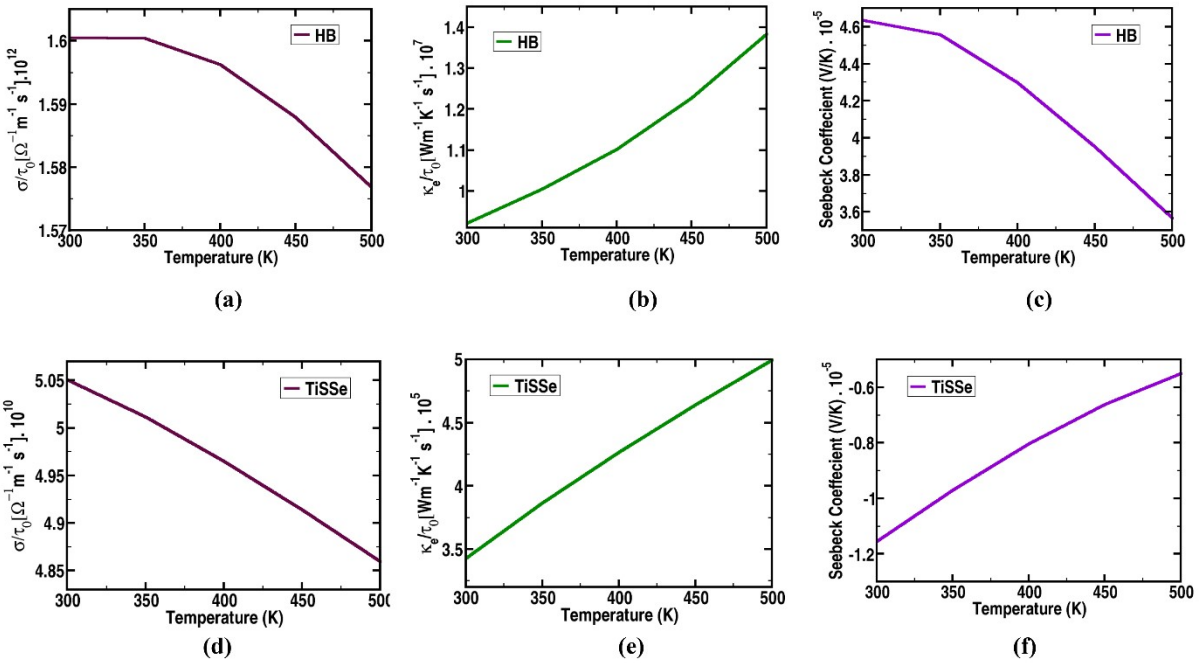

Fig. S4. Thermoelectric properties of constituent monolayers: **(a, d)** Electrical conductivity, **(b, e)** Thermal conductivity, and **(c, f)** Seebeck coefficient of pristine H-borophene, and Janus TiSSe monolayer, respectively.

In **Fig. S4 (a-c),** it is shown that H-borophene exhibits extremely high electrical conductivity (~1.60 × 10^{12} S/m at 300 K), confirming its metallic character and strong carrier mobility. The Seebeck coefficient is small and positive (~+4.63 × 10^{-5} V/K at 300 K), indicating hole-dominated transport consistent with metallic behavior. The electronic thermal conductivity increases with temperature and reaches a maximum value of ~1.38 × 10^{7} W/m·K at 500 K, reflecting efficient electronic heat transport associated with high carrier concentration.

In contrast, **Fig. S4 (d-f)** shows the Janus TiSSe monolayer exhibiting lower electrical conductivity (~5.05 × 10^{10} S/m at 300 K), suggesting reduced carrier density relative to H-borophene. Its Seebeck coefficient is small and negative (~−1.15 × 10^{-5} V/K at 300 K), indicating electron-dominated transport. The electronic thermal conductivity remains comparatively moderate (~4.99 × 10^{5} W/m·K at 500 K), consistent with its lower carrier mobility and weaker metallic response.

Overall, both monolayers exhibit metallic transport characteristics with small Seebeck coefficients. However, H-borophene demonstrates higher electrical and electronic thermal conductivities.